Pergamon

Int. J. Solids Structures Vol. 34, No. 27, pp. 3517–3540, 1997

0020-7683/97 $17.00 + .00

PII: S0020-7683(96)00185-0

MATERIALS WITH FLUID-FILLED PORES OF VARIOUS SHAPES: EFFECTIVE ELASTIC PROPERTIES AND FLUID PRESSURE POLARIZATION

B. SHAFIRO and M. KACHANOV
Department of Mechanical Engineering, Tufts University, Medford, MA, 02155 U.S.A.

(*Received* 8 *February* 1996; *in revised form* 12 *July* 1996)

Abstract—Three-dimensional solids with ellipsoidal pores of various shapes filled with compressible fluid are analyzed in the "undrained" approximation. Fluid pressures in cavities, induced by externally applied loads, depend on cavity shapes and cavity orientations with respect to the applied loads. This phenomenon ("pressure polarization") is coupled with the overall elastic response. The analysis covers mixtures of cavities of diverse shapes and arbitrary orientational distributions. Identification of the proper parameters of cavity density plays the key role in the analysis. © 1997 Elsevier Science Ltd.

1. FORMULATION OF THE PROBLEM

We consider a linear elastic solid containing pores of various shapes filled with non-viscous compressible fluid. The externally applied stress $\boldsymbol{\sigma}$ induces fluid pressures in cavities that depend on cavity orientations with respect to $\boldsymbol{\sigma}$, as well as on cavity shapes. This *pressure polarization* (different fluid pressures in different cavities) is coupled with stress interactions between cavities and with the overall elastic response of the material.

The problem of effective elastic properties of materials with fluid-filled pores was examined by O'Connell and Budiansky (1974) and Budiansky and O'Connell (1976) in the special case of pores' geometry—narrow, crack like cavities. Their analysis was limited to random orientations (isotropy) and the phenomenon of fluid pressure polarization was not discussed. We note that the applicability of their results is limited by the implicit assumption that all cavities have the same aspect ratios. In a number of works, the problem of pore pressure induced by the applied loads was addressed phenomenologically (without micromechanical analysis of pore shapes), with the porous space assumed interconnected; see Zimmerman (1991) for a review.

Kachanov (1993) considered an arbitrary orientational distribution of narrow crack-like cavities (anisotropic overall properties) and examined the fluid pressure polarization, as well as the impact of fluid on stress interactions between cracks. However, real materials may contain defects of more general shapes; moreover, they often contain *mixtures* of diverse defect shapes. Additional complicating factors are that the orientational distribution may be *non-random*, giving rise to anisotropy of the overall response, and that some of the pores may be "dry" or filled with fluid only partially. Figure 1 (salt water ice with inclusion of saline water) provides an illustration.

The present work gives a general 3-D analysis that covers fluid-filled pores of arbitrary ellipsoidal shapes. In particular, *mixtures* of cavities of diverse shapes (pores + cracks, etc.), relevant for real microstructures, are considered. Some preliminary results of the present study were reported by Kachanov *et al.* (1995).

The *undrained* approximation is assumed in the present work: the fluid mass in each cavity is constant. If the matrix allows fluid diffusion, this approximation corresponds to the "short time" response. In the opposite, "fully drained", limit, the effective response coincides with that of the dry solid, see Kachanov *et al.* (1994). Thus, the undrained approximation considered in the present work and the results for a dry material provide *bounds for the time-dependent effective moduli* in presence of diffusion.

One of the key issues is the identification of *proper parameters of cavity density*. We call the density parameter *proper*, if it correctly takes the individual defect contributions (with proper relative weights). Such parameters are necessary: only in their terms can the results for mixtures of diverse cavity shapes and for various orientational distributions be expressed. They are also convenient: the results cover all cavity shapes and orientational distributions in a *unified* way. Another advantage of the proper density parameters is that their identification establishes the *overall anisotropy* due to various defects (as determined by the symmetry of the tensorial density parameter). We show that these parameters are implied by the structure of the elastic potential.

The problem can be represented as a superposition of the sub-problems of Fig. 2:

(a) matrix containing a cavity loaded at its boundary by traction $\boldsymbol{\sigma}\cdot\mathbf{N}$, where $\boldsymbol{\sigma}$ is the uniform stress field at infinity and $\mathbf{N}$ is the outward to the material (inside the cavity) unit normal to the boundary;

(b) matrix with a cavity loaded at the boundary by traction $-\boldsymbol{\sigma}\cdot\mathbf{N}$; stresses vanish at infinity;

(c) same as (b) but with tractions $-q\mathbf{N}$ normal to the boundary, where q is the (yet unknown) fluid pressure in the cavity (assumed positive when compressive). Note that fluid pressure q is to be understood as a response to $\boldsymbol{\sigma}$. If a certain "background" pressure at $\boldsymbol{\sigma}=0$ is present, then q represents its change due to $\boldsymbol{\sigma}$.

Thus, the problem reduces to the one of a *dry* cavity with additional tractions $-q\mathbf{N}$.

We start with the usual representation of the overall strain per volume V of a linear elastic solid with stress $\boldsymbol{\sigma}$ at infinity and containing a cavity as a sum

$$\boldsymbol{\varepsilon}=\mathbf{S}^0:\boldsymbol{\sigma}+\Delta\boldsymbol{\varepsilon} \tag{1}$$

where $\mathbf{S}^0$ is the compliance tensor of the matrix; a colon denotes contraction over two indices. The additional strain due to cavity is

$$\Delta\boldsymbol{\varepsilon}=-\frac{1}{2V}\int_{\Gamma}(\mathbf{uN}+\mathbf{Nu})\,d\Gamma \tag{2}$$

where $\mathbf{u}$ denotes displacements of the cavity boundary Γ, and $\mathbf{uN}$, $\mathbf{Nu}$ denote dyadic (tensor) products of two vectors. The representation (2) follows from application of the divergence theorem to a strained solid with a cavity (it is an immediate consequence of a footnote remark of Hill, 1963 and was used in the explicit form by a number of authors, see, for example, Vavakin and Salganik, 1975).

Due to linearity of the system, $\Delta\boldsymbol{\varepsilon}$ per volume V is a linear function of $\boldsymbol{\sigma}$ and hence can be written as

$$\Delta\boldsymbol{\varepsilon}=\mathbf{H}:\boldsymbol{\sigma} \tag{3}$$

where the fourth rank tensor $\mathbf{H}$ is the *cavity compliance tensor* (possessing the usual symmetries $H_{ijkl}=H_{jilk}=H_{klij}$ implied by the existence of elastic potential). The $\mathbf{H}$-tensors were found for a number of 2-D shapes (ellipses, polygons) by Kachanov (1993) and Tsukrov and Kachanov (1993) and, for 3-D ellipsoids, by Kachanov *et al.* (1994).

For a *fluid-filled* cavity, the superposition of Fig. 2 reduces the analysis to the case of a *dry* cavity, by adding hydrostatic stress $q\mathbf{I}$ to $\boldsymbol{\sigma}$ in (3) ($\mathbf{I}$ is a unit tensor). The problem is thus reduced to finding fluid pressure q induced by $\boldsymbol{\sigma}$. In order to find q, we first relate it to the change in fluid density η (with respect to the reference density η_0 prior to application of $\boldsymbol{\sigma}$) through a constitutive equation for the fluid. For simplicity, we assume that the fluid is linearly compressible (κ is the fluid compressibility):

Fig. 1. Microstructure of salt water ice containing inclusions of saline water. (Courtesy of E. Gratz and E. Schulson, Dartmouth College.)

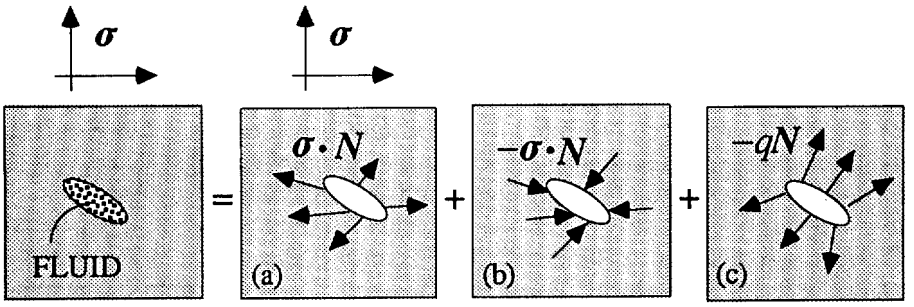

Fig. 2. Stress superposition for a solid with a fluid-filled cavity.

$$\Delta\eta/\eta_0 (= -\Delta V_{cav}/V_{cav}) = \kappa q. \tag{4}$$

Then, expressing the relative change of cavity volume $\Delta V_{cav}/V_{cav}$ in terms of compliance **H** of the dry cavity, we have:

$$\frac{V}{V_{cav}} tr(\mathbf{H}:\boldsymbol{\sigma}) + q\left[\frac{V}{V_{cav}} tr(\mathbf{H}:\mathbf{I}) - \frac{3(1-2\nu_0)}{E_0}\right] = -\kappa q \tag{5}$$

where the first term of the left-hand side corresponds to the sum of subproblems (a) and (b) of Fig. 2 and the second term to the subproblem (c). Equation (5) determines q as a linear function of $\boldsymbol{\sigma}$.

2. FLUID PRESSURE INDUCED BY A REMOTELY APPLIED STRESS IN A SINGLE ELLIPSOIDAL CAVITY

Fluid pressure q induced in a single cavity, being a linear function of remotely applied stress $\boldsymbol{\sigma}$, can be characterized by dimensionless second rank *pressure polarization tensor* **Q**:

$$q = \mathbf{Q}:\boldsymbol{\sigma} = Q_{ij}\sigma_{ij}. \tag{6}$$

Tensor **Q** is symmetric (it is defined by (6) to within its antisymmetric part, which can, therefore, be set equal to zero). **Q** depends on the geometry of the cavity and on its orientation with respect to $\boldsymbol{\sigma}$. For a *general ellipsoid* (with axes $2a_1, 2a_2, 2a_3$ aligned with unit vectors **l**, **m**, **n**, correspondingly), the results of Kachanov *et al.* (1994) for the **H**-tensor of a dry cavity, combined with equation (5), yield

$$\mathbf{Q} = -\frac{1}{1+\delta}\frac{1}{R}[R_1\mathbf{ll} + R_2\mathbf{mm} + R_3\mathbf{nn}] \tag{7}$$

where the dimensionless coefficients R_1, R_2, R_3 characterize the ellipsoid's geometry and are the following combinations of **H**-components (the latter are expressed in terms of Eshelby's tensor, see Appendix A): $R_1 = (VE_0/V_{cav})(H_{1111} + H_{1122} + H_{3311})$, $R_2 = (VE_0/V_{cav})(H_{1122} + H_{2222} + H_{2233})$, $R_3 = (VE_0/V_{cav})(H_{3311} + H_{2233} + H_{3333})$, and $R = R_1 + R_2 + R_3$. Note that R/E_0 characterizes the *compressibility* of a dry cavity: its relative volume change under the hydrostatic loading P is equal to PR/E_0 (in the text to follow, E_0 and ν_0 denote Young's modulus and Poisson's ratio of the matrix).

As seen from (7), the sensitivity of fluid pressure q to the applied stress $\boldsymbol{\sigma}$ depends on the dimensionless parameter that plays the key role in the analysis:

$$\delta = \frac{\kappa E_0 - 3(1-2\nu_0)}{R} = \frac{\kappa - C_0}{C_p} \tag{8}$$

where $C_p = R/E_0$ is the compressibility of a dry pore and $C_0 = 3(1-2\nu_0)/E_0$ is the compressibility of the matrix. Parameter δ incorporates the physical parameters—the matrix stiffness and the compressibility of the fluid—and the cavity geometry. As seen in the text to follow, δ determines the strength of coupling between fluid pressures in cavities and the overall elastic response. In the limit of a highly compressible fluid ("air") or a very stiff matrix, δ is large and $\boldsymbol{\sigma}$ produces almost no change in q; for an incompressible fluid, or a very soft matrix, δ is negative and the pressure change is maximal. The case when fluid and matrix compressibilities coincide ($\kappa = C_0$ so that $\delta = 0$) corresponds to "absence" of inhomogeneity for the hydrostatic loading. If the externally applied load is imagined as "carried" partially by the matrix and partially by the fluid, then δ determines their relative shares in carrying the load. This parameter generalizes the one introduced by O'Connell and Budiansky (1974) and Budiansky and O'Connell (1976) for the special case of a crack to general ellipsoidal cavities.

In the case of a *spheroid* ($a_1 = a_2 \equiv a$),

$$\mathbf{Q} = -\frac{1}{1+\delta}\frac{1}{R}(B_1\mathbf{nn} + B_2\mathbf{I}) \tag{9}$$

where $\mathbf{n}$ is a unit vector along the axis of symmetry of the spheroid and B_1, B_2, $R = 9A_1 + 3A_2 + 3A_3 + A_4 + A_5$ are combinations of Eshelby's tensor components (see Appendix A), which, for a spheroid, are expressed in elementary functions. Coefficients B_1/R and B_2/R depend on the aspect ratio $\zeta = a_3/a$ of the spheroid and on ν_0 (Fig. 3). The first term in (9) is orientation-dependent; coefficient B_1/R vanishes for a sphere. The second term is orientation-independent; coefficient B_2/R vanishes for a crack.

In the simplest case of a *sphere*, $R = 9(1-\nu_0)/2$ and

$$\delta = \frac{2}{9}\frac{\kappa E_0 - 3(1-2\nu_0)}{1-\nu_0}, \quad \mathbf{Q} = -\frac{1}{3(1+\delta)}\mathbf{I}. \tag{10}$$

We now consider three special cases of spheroid's geometry: narrow, crack-like cavity, somewhat deformed sphere and needle-shaped cavity.

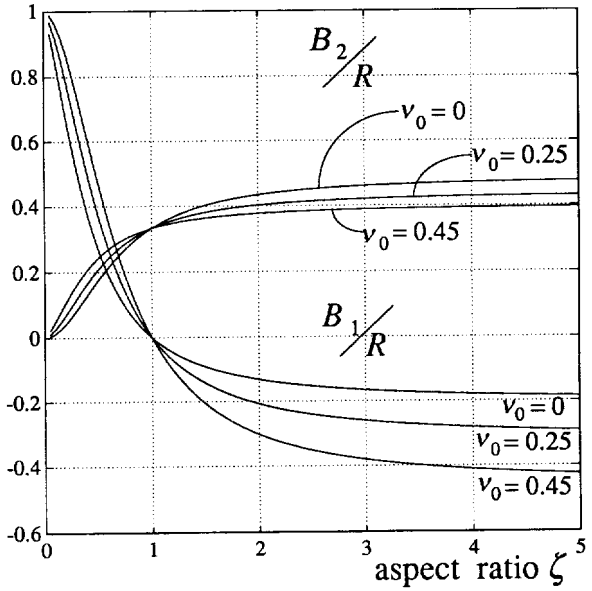

Fig. 3. Two coefficients, B_1/R and B_2/R, entering pressure polarization tensor $\mathbf{Q}$ for a spheroidal cavity, as functions of the aspect ratio ζ.

(1) *Narrow, crack-like spheroidal cavity* ($\zeta = a_3/a \ll 1$). In this case, $R = 4(1-\nu_0^2)/(\zeta\pi)$ and

$$\delta = \zeta\frac{\pi}{4(1-\nu_0^2)}[\kappa E_0 - 3(1-2\nu_0)], \quad \mathbf{Q} = -\frac{1}{1+\delta}\mathbf{nn} \tag{11}$$

when $\mathbf{n}$ is a unit normal to the crack. As seen from (11), the sensitivity of fluid pressure to applied loads is higher for thinner cavities (smaller ζ), provided the fluid compressibility κ is larger than the matrix compressibility C_0. In the opposite case $\kappa < C_0$, the mentioned sensitivity is lower for thinner cavities.

(2) *Somewhat deformed sphere* ($\zeta = a_3/a$; $|1-\zeta| \ll 1$). Retaining only the terms of the first order in $(1-\zeta)$, we find that the cavity compressibility coincides with the one of a perfect sphere of the same volume. Thus, $R = R_{\text{sphere}}$, $\delta = \delta_{\text{sphere}}$. Tensor $\mathbf{Q}$ is expressed as follows:

$$\mathbf{Q} = -\frac{1}{1+\delta}\frac{1}{3}\left\{\mathbf{I} - (1-\zeta)\frac{2(1+\nu_0)}{7-5\nu_0}(\mathbf{I}-3\mathbf{nn})\right\}. \tag{12}$$

In the case of hydrostatic loading $\boldsymbol{\sigma}$, the resulting fluid pressure response q coincides with the one for a sphere, i.e., the perturbation manifests itself only in terms of the second order in $1-a_3/a$.

(3) *Needle-shaped spheroidal cavity* ($\zeta = a_3/a \gg 1$). In this case, $R = 5-4\nu_0$ and

$$\delta = \frac{\kappa E_0 - 3(1-2\nu_0)}{5-4\nu_0}, \quad \mathbf{Q} = -\frac{1}{1+\delta}\frac{1}{5-4\nu_0}[-(1+\nu_0)\mathbf{nn} + (2-\nu_0)\mathbf{I}]. \tag{13}$$

In contrast with the case of crack-like cavity, δ does not depend on ζ, i.e., it is independent of the cavity geometry.

Returning now to the case of general ellipsoidal cavity, we observe that for *hydrostatic loading* $\boldsymbol{\sigma} = -P\mathbf{I}$, the fluid pressure induced in the cavity is

$$q = \frac{1}{1+\delta}P = \frac{C_p}{C_p+\kappa-C_0}P \tag{14}$$

recovering Skempton's coefficient $B = C_p/(C_p+\kappa-C_0)$ in the form obtained by Zimmerman (1991), for the special case of the spheroidal geometry. The dependence of q on the cavity shape is expressed only through the compressibility C_p of a dry cavity.

3. FLUID PRESSURE POLARIZATION. PRESSURE AMPLIFICATION IN FLUID INCLUSIONS

The dependence of fluid pressure q on applied stress $\boldsymbol{\sigma}$ is characterized by polarization tensor $\mathbf{Q}$ that describes, in particular, the dependence of q on the cavity orientation with respect to $\boldsymbol{\sigma}$. This orientational dependence of q is illustrated in Fig. 4 for the case of a uniaxial stress T oriented at different angles φ to the symmetry axis of a spheroid.

In a solid with *many* fluid-filled cavities, the fluid pressures will be different for differently oriented cavities, even if they have identical shapes. This phenomenon can be called *pressure polarization*. Since fluid pressures in cavities affect the displacements of cavity boundaries, the pressure polarization is coupled with the effective elastic properties.

Note that, in the presence of fluid diffusion in the matrix, the differences between fluid pressures in different cavities vanish with time, and, in the "long time" limit ("fully drained" approximation) the effective response coincides with the one of a *dry* material, studied, for cavities of various shapes, by Kachanov *et al.* (1994).

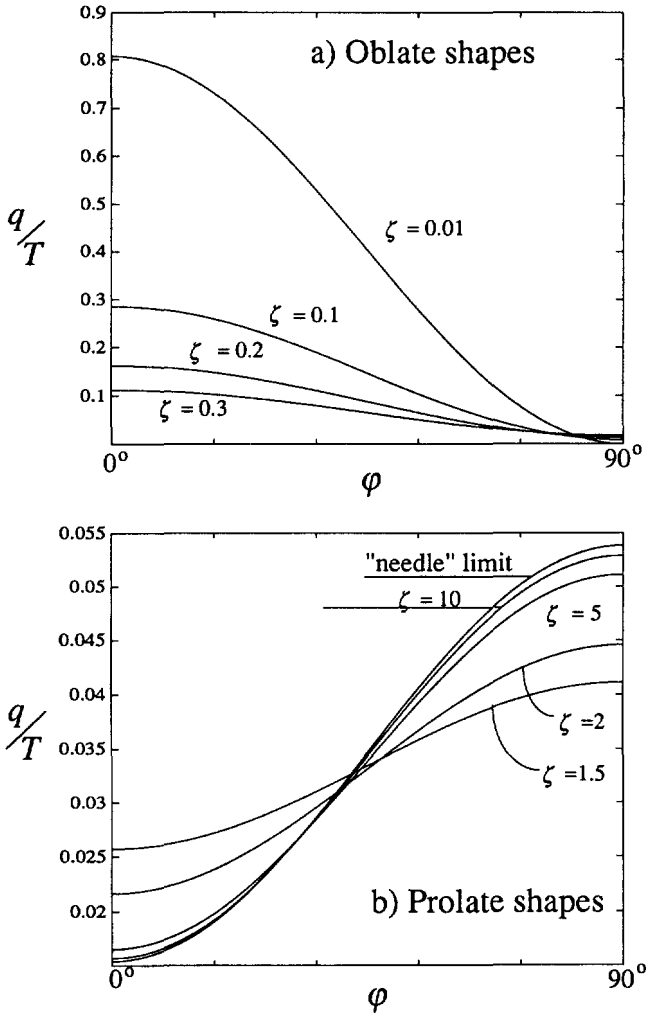

Fig. 4. Fluid pressure q induced in a spheroidal cavity by a uniaxial loading $-T$, as a function of orientation of the spheroid (φ is the angle between the cavity symmetry axis and the direction of compression) for several aspect ratios ζ. The material parameters correspond to granite ($E_0 = 6 \times 10^4$ MPa, $\nu_0 = 0.25$) filled with water ($\kappa = 0.5 \times 10^{-3}$ MPa^{-1}). (a) Oblate shapes. (b) Prolate shapes.

We also remark that, since the developed theory is linear, it applies, formally speaking, to both compressive and tensile loadings. However, its applicability in the case of tensile loading is limited by the onset of fluid cavitation.

Another interesting phenomenon is that fluid inclusions may act as "*pressure amplifiers*". Pressure q in a fluid inclusion induced by applied hydrostatic pressure P can *exceed* P in the case of undrained compression, provided the fluid compressibility is lower than the matrix one ($\kappa < C_0$). For an incompressible fluid ($\kappa = 0$), the factor relating q to P is always >1 (except for the case of an incompressible matrix, $\nu_0 = 1/2$, when q is exactly equal to P). This effect is very sensitive to Poisson's ratio ν_0 and is maximal when $\nu_0 = 0$, i.e., when the constraint provided by the matrix against the cavity volume change is maximal (Fig. 5). For the *spherical* shape this amplifying factor is maximal and may be as high as 3 (at $\kappa = 0$, $\nu_0 = 0$); it is almost as high (≈ 2.5) in the limit of a needle. For a narrow, crack-like spheroidal cavity with an aspect ratio $\zeta \ll 1$, this factor is $[1 - 3\pi\zeta/4]^{-1} = 1 + 2.36\zeta$. Thus, the sensitivity of q to the hydrostatic loading is highest for a sphere, somewhat lower for a needle and rapidly drops for oblate shapes (Fig. 5).

In the case of non-hydrostatic loading $\boldsymbol{\sigma}$, the "stress amplification" may also take place for certain $\boldsymbol{\sigma}$'s, provided $\kappa < C_0$. This effect occurs, for example, in the cases of uniaxial loading normal to a crack-like cavity or a 2-D hydrostatic stress in the plane normal to a needle-shaped cavity.

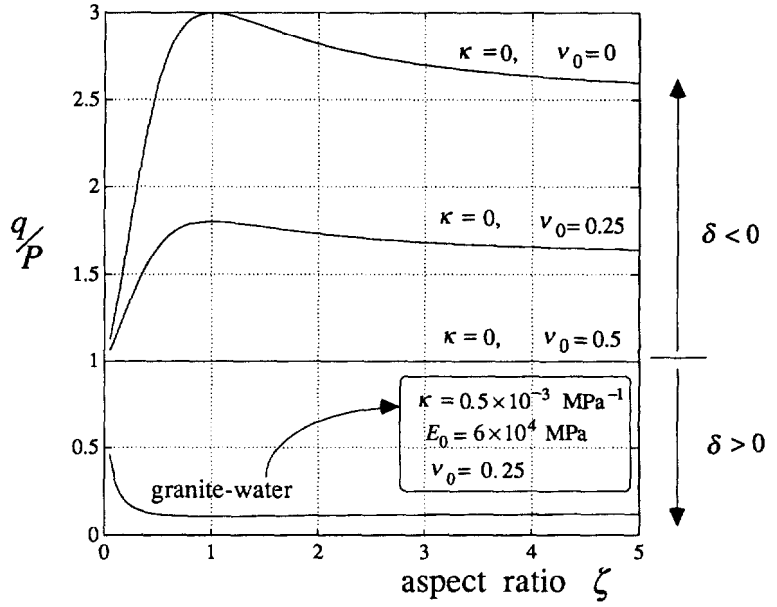

Fig. 5. Fluid pressure q in a spheroidal cavity induced by remotely applied hydrostatic pressure P. Dependence of the q-P diagram on the aspect ratio of the cavity. Note strong dependence on the Poisson's ratio of the matrix.

4. COMPLIANCE TENSORS OF FLUID-FILLED CAVITIES

As follows from the superposition of Fig. 2, the compliance tensor $\tilde{\mathbf{H}}$ of a fluid-filled cavity is a sum of $\mathbf{H}$ for a dry cavity and the correctional term $\Delta\mathbf{H}$ accounting for the fluid presence: $\tilde{\mathbf{H}} = \mathbf{H} + \Delta\mathbf{H}$. Correctional tensor $\Delta\mathbf{H}$ can be derived in terms of $\mathbf{H}$ and pressure polarization tensor $\mathbf{Q}$. Indeed, the superposition of Fig. 2 implies that

$$\Delta\boldsymbol{\varepsilon} = \Delta\boldsymbol{\varepsilon}^{\text{dry}} + \Delta\boldsymbol{\varepsilon}^{\text{fluid}} = \mathbf{H}:\boldsymbol{\sigma} + \mathbf{H}:(q\mathbf{I}) = \mathbf{H}:\boldsymbol{\sigma} + (\mathbf{H}:\mathbf{IQ}):\boldsymbol{\sigma} = \mathbf{H}:\boldsymbol{\sigma} + \Delta\mathbf{H}:\boldsymbol{\sigma} \tag{15}$$

so that, after the usual symmetrization of ΔH_{ijkl} with respect to $ij \leftrightarrow kl$, we obtain:

$$\Delta\mathbf{H} = \tfrac{1}{2}(\mathbf{QH}:\mathbf{I} + \mathbf{H}:\mathbf{IQ}) \quad \text{or} \quad \Delta H_{ijkl} = \tfrac{1}{2}(Q_{ij}H_{klmn}\delta_{mn} + H_{ijmn}\delta_{mn}Q_{kl}). \tag{16}$$

With $\mathbf{Q}$ given by (7–12), we thus express $\Delta\mathbf{H}$ in terms of dry cavity compliance $\mathbf{H}$ and parameter δ.

For *general ellipsoid*, $\mathbf{H}$-tensor has the form:

$$\begin{aligned}\mathbf{H} = {} & H_{1111}\mathbf{llll} + H_{2222}\mathbf{mmmm} + H_{3333}\mathbf{nnnn} + H_{1122}(\mathbf{llmm} + \mathbf{mmll}) \\ & + H_{2233}(\mathbf{mmnn} + \mathbf{nnmm}) + H_{3311}(\mathbf{nnll} + \mathbf{llnn}) + H_{1212}(\mathbf{lm} + \mathbf{ml})(\mathbf{lm} + \mathbf{ml}) \\ & + H_{2323}(\mathbf{mn} + \mathbf{nm})(\mathbf{mn} + \mathbf{nm}) + H_{3131}(\mathbf{nl} + \mathbf{ln})(\mathbf{nl} + \mathbf{ln})\end{aligned} \tag{17}$$

where H_{ijkl} are expressed in terms of Eshelby's tensor (see Appendix A). Utilizing this result, along with (7) and (16), we derive $\Delta\mathbf{H}$ in the form:

$$\begin{aligned}\Delta\mathbf{H} = {} & -\frac{1}{1+\delta}\frac{V_{cav}}{V}\frac{1}{E_0}\frac{1}{R}\{R_1^2\mathbf{llll} + R_2^2\mathbf{mmmm} + R_3^2\mathbf{nnnn} \\ & + R_1R_2(\mathbf{llmm} + \mathbf{mmll}) + R_2R_3(\mathbf{mmnn} + \mathbf{nnmm}) + R_1R_3(\mathbf{nnll} + \mathbf{llnn})\}\end{aligned} \tag{18}$$

where the key role played by parameter δ is again seen.

For a dry *general spheroid* ($\mathbf{n}$ is a unit vector along the symmetry axis):

$$\mathbf{H} = \frac{V_{cav}}{V}\frac{1}{E_0}\left[A_1\mathbf{II} + A_2\mathbf{J} + \frac{A_3}{2}(\mathbf{nnI}+\mathbf{Inn}) + A_4\mathbf{nIn} + A_5\mathbf{nnnn}\right] \tag{19}$$

where coefficients A_i are given in Appendix A and $\mathbf{J}$ is the fourth rank isotropic tensor with components $J_{ijkl} = \delta_{ik}\delta_{jl} + \delta_{il}\delta_{jk}$. In this case,

$$\Delta\mathbf{H} = -\frac{1}{1+\delta}\frac{V_{cav}}{V}\frac{1}{E_0}[B_3\mathbf{II} + B_4(\mathbf{nnI}+\mathbf{Inn}) + B_5\mathbf{nnnn}] \tag{20}$$

where coefficients B_i are given in Appendix A. Thus, the overall compliance tensor of a fluid-filled general spheroid has the form

$$\hat{\mathbf{H}} = \frac{V_{cav}}{V}\frac{1}{E_0}\left[\left(A_1 - \frac{B_3}{1+\delta}\right)\mathbf{II} + A_2\mathbf{J} + \left(\frac{A_3}{2} - \frac{B_4}{1+\delta}\right)(\mathbf{nnI}+\mathbf{Inn}) + A_4\mathbf{nIn} + \left(A_5 - \frac{B_5}{1+\delta}\right)\mathbf{nnnn}\right]. \tag{21}$$

The first two terms in the brackets are orientation-independent (the isotropic strain response of the cavity) and the remaining terms contain $\mathbf{n}$ and are orientation-dependent.

In the simplest case of a *sphere*, the orientation-dependent terms vanish (coefficients A_3, A_5, B_4, B_5 vanish) and

$$\mathbf{H} = \frac{V_{cav}}{V}\frac{3(1-\nu_0)}{2(7-5\nu_0)E_0}[10(1+\nu_0)\mathbf{J} - (1+5\nu_0)\mathbf{II}], \quad \Delta\mathbf{H} = -\frac{1}{1+\delta}\frac{V_{cav}}{V}\frac{(1-\nu_0)}{2E_0}\mathbf{II} \tag{22}$$

$$\hat{\mathbf{H}} = \frac{V_{cav}}{V}\frac{3(1-\nu_0)}{2E_0}\left\{\frac{10(1+\nu_0)}{7-5\nu_0}\mathbf{J} - \left[\frac{1+5\nu_0}{7-5\nu_0} + \frac{1}{1+\delta}\frac{1}{3}\right]\mathbf{II}\right\}. \tag{23}$$

We now consider three special cases of spheroid's geometry: two limiting cases (crack-like cavity and a needle) and the case of a slightly deformed sphere. For a crack-like cavity and for a needle, we neglect terms of the first order in a small parameter ζ for a crack and terms of the second order in a small parameter ζ^{-1} for a needle; in the case of a deformed sphere, the first order correction to the spherical shape is derived. The range of applicability of the results for these special geometries is determined by requiring that the maximum (taken over non-zero H_{ijkl}) of the ratio $|(H^{\text{exact}}_{ijkl} - H^{\text{approx}}_{ijkl})/H^{\text{exact}}_{ijkl}|$ is sufficiently small. This requirement guarantees that each component $\Delta\varepsilon_{ij}$ of the additional strain due to cavity is well approximated by the asymptotic expression, for all stress states σ_{ij}.

(1) For a *crack-like* spheroidal cavity (aspect ratio $\zeta = a_3/a \ll 1$), the orientation-independent terms vanish and we have

$$\mathbf{H} = \frac{a^3}{V}\frac{16(1-\nu_0^2)}{3(1-\nu_0/2)E_0}\left(\mathbf{nIn} - \frac{\nu_0}{2}\mathbf{nnnn}\right), \quad \Delta\mathbf{H} = -\frac{a^3}{V}\frac{16(1-\nu_0^2)}{3E_0}\frac{1}{1+\delta}\mathbf{nnnn} \tag{24}$$

$$\hat{\mathbf{H}} = \frac{a^3}{V}\frac{16(1-\nu_0^2)}{3(1-\nu_0/2)E_0}\left\{\mathbf{nIn} - \left[\frac{\nu_0}{2} + \frac{1}{1+\delta}\left(1-\frac{\nu_0}{2}\right)\right]\mathbf{nnnn}\right\}. \tag{25}$$

The range of applicability of these asymptotic expressions depends on Poisson's ratio ν_0 and on parameter δ. For $\nu_0 = 0.25$ and for a dry cavity, these results apply with errors of less than 5% and 10% for the aspect ratios $\zeta < 0.05$ and $\zeta < 0.1$ correspondingly.

(2) For a *somewhat deformed sphere* ($|1-\zeta| \ll 1$) we obtain

$$\mathbf{H} = \frac{V_{cav}}{V}\frac{3(1-\nu_0)}{2(7-5\nu_0)E_0}\left\{10(1+\nu_0)\mathbf{J} - (1+5\nu_0)\mathbf{II} + (1-\zeta)\frac{2(1+\nu_0)}{7(7-5\nu_0)}[-2(5-7\nu_0)\mathbf{J} + 2(17-35\nu_0)\mathbf{II} - 3(17-35\nu_0)(\mathbf{nnI}+\mathbf{Inn}) - 60(5-7\nu_0)\mathbf{nIn}]\right\} \quad (26)$$

$$\Delta\mathbf{H} = -\frac{1}{1+\delta}\frac{V_{cav}}{V}\frac{3(1-\nu_0)}{2E_0}\left\{\frac{1}{3}\mathbf{II} + (1-\zeta)\frac{2(1+\nu_0)}{7-5\nu_0}\left[-\frac{2}{3}\mathbf{II} + (\mathbf{nnI}+\mathbf{Inn})\right]\right\}. \quad (27)$$

The range of applicability of these asymptotic expressions depends on Poisson's ratio ν_0 and on parameter δ. For $\nu_0 = 0.25$ and for a dry cavity, these results apply with errors of less than 5% and 10% for the aspect ratios $0.6 < \zeta < 1.65$ and $0.5 < \zeta < 2$ correspondingly.

(3) In the limit of a *needle-shaped* cavity (aspect ratio $\zeta = a_3/a \gg 1$),

$$\mathbf{H} = \frac{V_{cav}}{V}\frac{1}{E_o}[-(1-2\nu_0^2)\mathbf{II} + 4(1-\nu_0^2)\mathbf{J} + (1-2\nu_0)(1+\nu_0)(\mathbf{nnI}+\mathbf{Inn}) - 4(1-2\nu_0)(1+\nu_0)\mathbf{nIn} - 2\nu_0(1+\nu_0)\mathbf{nnnn}] \quad (28)$$

$$\Delta\mathbf{H} = -\frac{1}{1+\delta}\frac{V_{cav}}{V}\frac{1}{E_0}\frac{(2-\nu_0)(1+\nu_0)}{5-4\nu_0}\left[\frac{2-\nu_0}{1+\nu_0}\mathbf{II} - (\mathbf{nnI}+\mathbf{Inn}) + \frac{1+\nu_0}{2-\nu_0}\mathbf{nnnn}\right]. \quad (29)$$

The range of applicability of these asymptotic expressions strongly depends on Poisson's ratio ν_0 (the error increases with $\nu_0 \to 0$) and on parameter δ. For $\nu_0 = 0.25$ and for a dry cavity, these results apply with errors of less than 5% and 10% for the aspect ratios $\zeta > 12$ and $\zeta > 8$, correspondingly.

5. EFFECTIVE ELASTIC PROPERTIES OF A SOLID WITH FLUID-FILLED CAVITIES. PROPER PARAMETERS OF CAVITY DENSITY

We restrict the analysis to the approximation of non-interacting cavities (each cavity is placed in the externally applied stress $\boldsymbol{\sigma}$ and experiences no influence of neighbors). This approximation is of a fundamental importance: besides being rigorous for small cavity densities (provided the mutual positions of cavities are random), it constitutes a basic building block for various approximate schemes. Such schemes usually place *non-interacting* defects into some sort of "effective environment"—effective matrix (self-consistent, differential schemes) or effective stress (Mori-Tanaka's scheme). Therefore, the results of the present work can be rewritten in the framework of any of these schemes.

The effective elastic properties are best analyzed in terms of elastic potentials. Formulation in potentials has the conceptual advantage: it establishes the *proper cavity density parameters*—parameters that correctly take the individual defect contributions (with correct relative weights). Only in terms of such parameters can the effective properties be uniquely expressed.

Formulation in terms of proper density parameters yields the following advantages:

1. Identification of proper density parameters establishes *the overall anisotropy* for arbitrary statistics of cavity orientations and aspect ratios.

2. The effective moduli are obtained *in a unified way* for all orientational and aspect ratio distributions, including *mixtures* of defects of diverse shapes, that are typical for real microstructures.

3. The results do not degenerate in the cases when cavity volumes shrink to zero (cracks).

As follows from (1), the elastic potential in stresses (complementary energy density) $f(\boldsymbol{\sigma}) = (1/2)\boldsymbol{\sigma} : \boldsymbol{\varepsilon}(\boldsymbol{\sigma})$ can be represented as a sum

$$f(\boldsymbol{\sigma}) = f_0 + \Delta f \quad (30)$$

where $f_0 = (1/2E_0)[(1+\nu_0)tr(\boldsymbol{\sigma}\cdot\boldsymbol{\sigma}) - \nu_0(tr\boldsymbol{\sigma})^2]$ is the potential in absence of cavities and Δf is due to cavities. The problem of effective properties is thus reduced to finding Δf as a function of $\boldsymbol{\sigma}$. Effective compliances s_{ijkl} are then found from $\varepsilon_{ij} = \partial f/\partial\sigma_{ij} = s_{ijkl}\sigma_{kl}$.

The results of the present work can, of course, be reformulated in compliances, rather than potentials. We prefer the formulation in potentials, since it identifies the proper parameters of cavity density in the most transparent way.

Potential Δf has the form of a sum over all cavities:

$$\Delta f = \tfrac{1}{2}\boldsymbol{\sigma} : \Sigma\,\Delta\boldsymbol{\varepsilon}^{(k)} = \tfrac{1}{2}\boldsymbol{\sigma} : \Sigma\hat{\mathbf{H}}^{(k)} : \boldsymbol{\sigma} = \underbrace{\tfrac{1}{2}\boldsymbol{\sigma} : \Sigma\mathbf{H}^{(k)} : \boldsymbol{\sigma}}_{\Delta f_{dry}} + \tfrac{1}{2}\boldsymbol{\sigma} : \Sigma\,\Delta\mathbf{H}^{(k)} : \boldsymbol{\sigma} \tag{31}$$

and results of Section 4 for $\Delta\mathbf{H}^{(k)}$ can be utilized.

Structure of the potential identifies fourth rank tensor $\Sigma\hat{\mathbf{H}}^{(k)} = \Sigma(\mathbf{H}+\Delta\mathbf{H})^{(k)}$ as the proper general parameter of cavity density. This parameter may seem complex, but its complexity is unaviodable: it covers diverse situations (mixtures of diverse shapes, various orientational distributions) in a unified way. If the diversity is restricted, the parameter simplifies and may, possibly, be replaced by a second rank tensor or, in the case of isotropy, by one or two scalars.

Note that the density parameters are non-trivial, even in the simplest case of isotropy. For example, porosity (relative volume of cavities) is not an adequate parameter for randomly oriented general spheroids. For *fluid-filled* cavities, the density parameters reflect both cavity shapes and fluid compressibility. In the text to follow, these parameters are specialized for several cavity geometries and orientational distributions.

On the replacement of summation by integration

Summation over cavities can, for computational convenience, be replaced by integration over the cavity orientations, aspect ratios and sizes. For example, for spheroids characterized by orientations $\mathbf{n}$, aspect ratios ζ and cross-sectional radii a, the sums would have to be replaced by the following integrals:

$$\sum\hat{\mathbf{H}}^{(k)} \to \int_0^\infty \int_0^\infty \int_\Omega \hat{\mathbf{H}}(\mathbf{n},\zeta,a)P(\mathbf{n},\zeta,a)\,\mathrm{d}\Omega\,\mathrm{d}\zeta\,\mathrm{d}a \tag{32}$$

where Ω is a hemisphere and $P(\mathbf{n},\zeta,a)$ is a probability density function (which is not necessarily representable as a product $P_1(\mathbf{n})P_2(\zeta)P_3(a)$, since cavities of certain orientations may tend to be thinner and smaller than the ones of other orientations). We use a simpler notation of sums throughout this work. In the cases of parallel and fully random (isotropic) orientational distributions, calculations of sums are straightforward. In the cases of more complex statistics the transition (32) can always be done and may be convenient if the density function P is known.

We now specialize (31) for several specific cavity shapes. Setting fluid compressibility κ in the formulas below to ∞ (then $\delta^{(k)} = \infty$) or to 0 (then $\delta^{(k)} = -C_0/C_p^{(k)}$) corresponds to the limiting cases of a dry solid and of an incompressible fluid. If some of the cavities are dry (or only partially filled with fluid), then $\delta^{(k)} = \infty$ for them.

For the *general spheroids*,

$$\begin{aligned}\Delta f = \frac{1}{2E_0}\Bigg\{&\frac{1}{V}\sum\left[V_{cav}\left(A_1 - \frac{B_3}{1+\delta}\right)\right]^{(k)}(tr\boldsymbol{\sigma})^2 + \frac{1}{V}\sum[V_{cav}A_2]^{(k)}tr(\boldsymbol{\sigma}\cdot\boldsymbol{\sigma})\\ &+ (tr\boldsymbol{\sigma})\boldsymbol{\sigma} : \frac{1}{V}\sum\left[V_{cav}\left(A_3 - \frac{2B_4}{1+\delta}\right)\mathbf{nn}\right]^{(k)} + (\boldsymbol{\sigma}\cdot\boldsymbol{\sigma}) : \frac{1}{V}\sum[V_{cav}A_4\mathbf{nn}]^{(k)}\\ &+ \boldsymbol{\sigma} : \frac{1}{V}\sum\left[V_{cav}\left(A_5 - \frac{B_5}{1+\delta}\right)\mathbf{nnnn}\right]^{(k)} : \boldsymbol{\sigma}\Bigg\}.\end{aligned} \tag{33}$$

The first two terms in the braces are expressed in stress invariants $tr\boldsymbol{\sigma}$ and $tr(\boldsymbol{\sigma}\cdot\boldsymbol{\sigma})$ and thus

characterize the isotropic response, independent of cavity orientations. They vanish for cracks. The last three terms are orientation-dependent; they vanish for spheres.

The structure of Δf implies the proper cavity density parameters as the terms that enter (33) in products with stresses. They identify the individual k-th cavity contributions, and thus take contributions with correct "relative weights". There are five of them: two scalars, two second rank tensors and a fourth rank tensor. The effective properties are expressed in their terms in a unified way with respect to all statistics of orientations and aspect ratios. In the text to follow, we specialize them to simpler parameters having transparent physical meaning for various special cases (cracks, needles, spheres and somewhat deformed spheres).

We first consider the case of overall isotropy (randomly oriented spheroids, with aspect ratios and sizes uncorrelated with orientations). We start with a general remark on the structure of the isotropic elastic potential and its applications for the parameters of cavity density. Any isotropic elastic potential, being expressed in stress invariants, is a sum of two terms, $(tr\boldsymbol{\sigma})^2$ and $tr(\boldsymbol{\sigma}\cdot\boldsymbol{\sigma})$; therefore, we have no more than two scalar density parameters—coefficients at these terms. Indeed, in the case of isotropy the second and fourth rank tensors $(1/V)\Sigma[\ ]^{(k)}$ entering the last three terms of (33) have to be isotropic and hence can be found as outlined in Appendix B. This yields

$$\Delta f = \frac{1}{30E_0}[p_1(tr\boldsymbol{\sigma})^2 + p_2 tr(\boldsymbol{\sigma}\cdot\boldsymbol{\sigma})]. \tag{34}$$

Therefore, the two scalars

$$p_1 = \frac{1}{V}\sum\left[\left(D_1 - \frac{1}{1+\delta}D_2\right)V_{cav}\right]^{(k)}, \quad p_2 = \frac{1}{V}\sum\left[\left(D_3 - \frac{1}{1+\delta}D_4\right)V_{cav}\right]^{(k)} \tag{35}$$

(where $D_1 = 15A_1 + 5A_3 + A_5$, $D_2 = 15B_3 + 10B_4 + B_5$, $D_3 = 15A_2 + 5A_4 + 2A_5$, $D_4 = 2B_5$) are the proper density parameters. They combine the information on cavity shapes with physical parameters $\delta^{(k)}$ in a non-trivial way. Only in terms of these parameters can the effective isotropic elastic moduli be expressed in a unified way, for all mixtures of spheroids of diverse aspect ratios:

$$\frac{E_0}{E} = 1 + \frac{1}{15}(p_1 + p_2), \quad \frac{G_0}{G} = 1 + \frac{1}{30(1+\nu_0)}p_2. \tag{36}$$

Neither of the density parameters p_1, p_2 can be reduced to porosity $p = (1/V)\Sigma V_{cav}^{(k)}$. Thus, even in the case of isotropy, *porosity is not a proper parameter of cavity density*. It does become adequate in the case of spheres (as expected) and in the (less obvious) case of randomly oriented needles. Figure 6 illustrates relations (36) as functions of cavity shapes.

An interesting observation is that in the wide range of aspect ratios ζ (from about 0.7 to ∞) the curves of Fig. 6 are almost horizontal. This means that, at a given overall porosity p, the effective moduli in the case of random orientations are almost insensitive to cavity shapes in the mentioned range of ζ. This insensitivity holds for both dry and fluid-filled pores.

We now return to the general orientational distribution and examine several special cases of cavity geometries.

(1) *Spheres*. This simplest case is obviously isotropic and is therefore covered by potential (34). Both density parameters p_1 and p_2 are proportional to porosity $p = (1/V)\Sigma V_{cav}^{(k)}$, with constant proportionality coefficients (dependent on ν_0 and δ). Therefore, only one density parameter p remains and

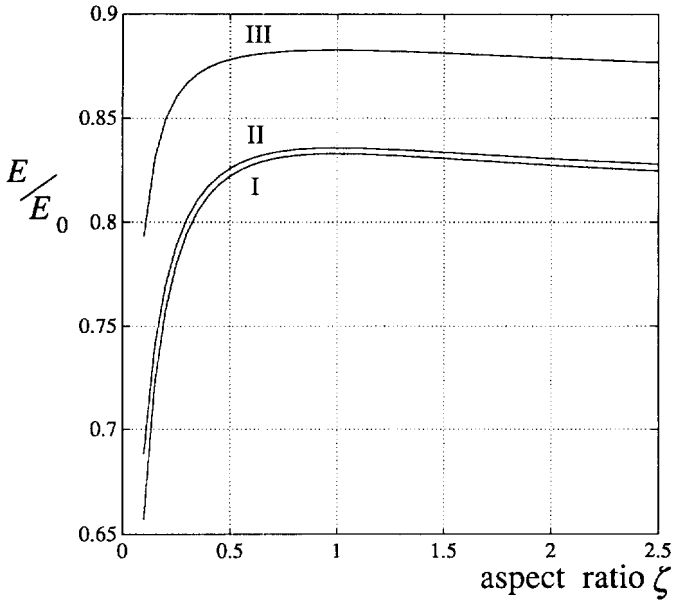

Fig. 6. Randomly oriented spheroidal cavities of identical aspect ratios ζ. Effective Young's modulus as a function of ζ (porosity is kept constant, $p = 0.1$). I—dry material; II—granite ($E_0 = 6 \times 10^4$ MPa, $\nu_0 = 0.25$) with cavities filled with water ($\kappa = 0.5 \times 10^{-3}$ MPa^{-1}); III—cavities filled with an incompressible fluid ($\kappa = 0$).

$$\Delta f = p\frac{3(1-\nu_0)}{4E_0}\left\{\frac{10(1+\nu_0)}{7-5\nu_0}tr(\boldsymbol{\sigma}\cdot\boldsymbol{\sigma}) - \left[\frac{1+5\nu_0}{7-5\nu_0} + \frac{1}{1+\delta}\frac{1}{3}\right](tr\boldsymbol{\sigma})^2\right\} \tag{37}$$

so that the effective isotropic moduli are:

$$\frac{E_0}{E} = 1+p\left[\frac{3(1-\nu_0)(9+5\nu_0)}{2(7-5\nu_0)} - \frac{1}{1+\delta}\frac{1-\nu_0}{2}\right], \quad \frac{G_0}{G} = 1+p\frac{15(1-\nu_0)}{2(7-5\nu_0)}. \tag{38}$$

As seen from (38), the presence of fluid does not affect the effective shear modulus ((38$_2$) does not contain δ).

(2) *Crack-like cavities.* The general result (33) reduces to

$$\Delta f = \underbrace{\frac{16(1-\nu_0^2)}{3(2-\nu_0)E_0}\left[(\boldsymbol{\sigma}\cdot\boldsymbol{\sigma}):\frac{1}{V}\sum(a^3\mathbf{nn})^{(k)} - \frac{\nu_0}{2}\boldsymbol{\sigma}:\frac{1}{V}\sum(a^3\mathbf{nnnn})^{(k)}:\boldsymbol{\sigma}\right]}_{\Delta f_{dry}}$$

$$-\frac{8(1-\nu_0^2)}{3E_0}\left[\boldsymbol{\sigma}:\frac{1}{V}\sum\left(\frac{a^3}{1+\delta}\mathbf{nnnn}\right)^{(k)}:\boldsymbol{\sigma}\right]. \tag{39}$$

The structure of this potential is quite instructive. Its first part (derived by Kachanov, 1980) corresponds to *dry* cracks. The second part (vanishing in the case of dry or partially filled cracks, or a highly compressible fluid, $\delta^{(k)} \to \infty$) is due to the presence of fluid. When $\delta^{(k)} = 0$ (either $\kappa = C_0$ or $\zeta^{(k)} \to 0$), Δf given by (39) reduces to the potential of a solid with cracks *constrained against the normal opening* but allowed to slide without friction (Kachanov, 1982, 1992).

The structure of the potential implies the following second and fourth rank tensors as the proper cavity density parameters:

$$\left.\begin{aligned} &\frac{1}{V}\sum(a^3\mathbf{nn})^{(k)} \equiv \boldsymbol{\alpha}, \quad \text{crack density tensor} \\ &\frac{1}{V}\sum(a^3\mathbf{nnnn})^{(k)} \end{aligned}\right\} \text{dry cracks}$$
$$\left.\begin{aligned} &\\ &\frac{1}{V}\sum\left(\frac{a^3}{1+\delta}\mathbf{nnnn}\right)^{(k)} \text{ accounts for fluid presence} \end{aligned}\right\}. \tag{40}$$

Remark. The two terms of (39) containing fourth rank tensors can, in principle, be reduced to one: $-[8(1-\nu_0^2)/3E_0]\boldsymbol{\sigma}:(1/V)\Sigma\{a^3[\nu_0/(2-\nu_0)+(1+\delta)^{-1}]\mathbf{nnnn}\}^{(k)}:\boldsymbol{\sigma}$. Then the number of proper cavity density parameters reduces to two (the two fourth rank tensors in (40) can be combined into one). However, the form (39) implying the three parameters (40) is preferable from the physical point of view, since it separates the "dry" part from the one due to fluid.

The exact potential (39) can be replaced by a simpler approximate expression, with reduced number of density parameters, as follows. In the "dry" part of Δf, the second term enters with a relatively small multiplier $\nu_0/2$ and can, therefore, be neglected in the first approximation (Kachanov, 1980). Then,

$$\Delta f \approx \frac{16(1-\nu_0^2)}{3(2-\nu_0)E_0}\left[(\boldsymbol{\sigma}\cdot\boldsymbol{\sigma}):\boldsymbol{\alpha}-(1-\nu_0/2)\boldsymbol{\sigma}:\frac{1}{V}\sum\left(\frac{a^3}{1+\delta}\mathbf{nnnn}\right)^{(k)}:\boldsymbol{\sigma}\right] \tag{41}$$

so that only two density parameters are sufficient: second rank crack density tensor $\mathbf{a}$ and the fourth rank tensor (40_3) accounting for the fluid presence.

In the case of *parallel* crack-like cavities (with unit normals $\mathbf{n} = \mathbf{e}_3$),

$$\Delta f = \frac{16(1-\nu_0^2)}{3(2-\nu_0)E_0}\left\{\rho\sigma_{3j}\sigma_{j3}-\left[\frac{\nu_0}{2}\rho+(1-\nu_0/2)\rho_1\right]\sigma_{33}^2\right\} \tag{42}$$

implying that, if $\mathbf{n}$ is fixed, the tensorial parameters (40) are replaced by two scalars

$$\rho = \frac{1}{V}\sum(a^3)^{(k)}, \quad \rho_1 = \frac{1}{V}\sum\left(\frac{a^3}{1+\delta}\right)^{(k)} \tag{43}$$

where the first one is the usual scalar crack density. The second density parameter ρ_1 differs from ρ in reducing the k-th crack contribution by the multiplier $(1+\delta^{(k)})^{-1}$ that characterizes the fluid influence. It affects only the coefficient at σ_{33}^2 (and does not affect coefficient at σ_{13}, σ_{23}): the presence of fluid reduces cracks' influence on the effective Young's modulus E_3 but does not affect their influence on *shear* modulus G_{13}.

The transversely isotropic effective moduli are expressed in terms of parameters ρ, ρ_1 in a unified way, with respect to all distributions of the aspect ratios $\zeta^{(k)}$ and sizes $a^{(k)}$:

$$\frac{E_0}{E_3} = 1+\frac{16}{3}(1-\nu_0^2)[\rho-\rho_1], \quad \nu_{31} = \frac{3\nu_0}{3+16(1-\nu_0^2)[\rho-\rho_1]}, \quad \frac{G_0}{G_{13}} = 1+\rho\frac{16(1-\nu_0)}{3(2-\nu_0)} \tag{44}$$

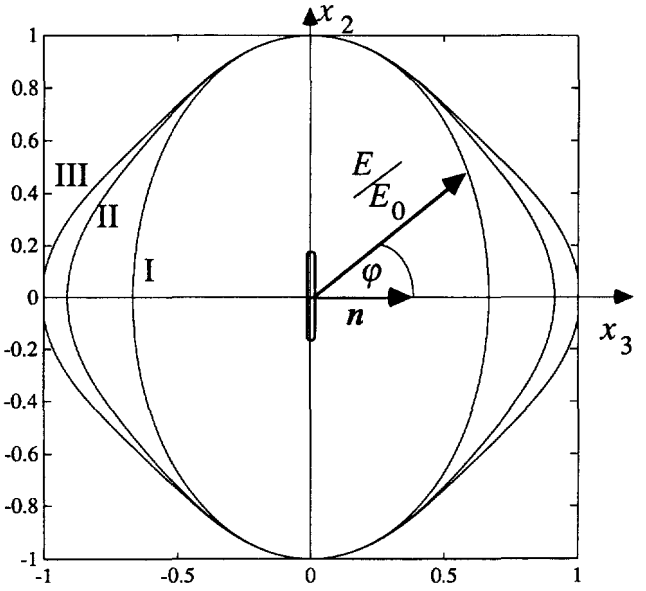

Fig. 7. Parallel narrow, crack-like spheroidal cavities with the aspect ratio $\zeta = 0.01$ (crack density parameter $\rho = 0.1$). Variation of the effective Young's modulus with direction. I—dry material; II—granite ($E_0 = 6 \times 10^4$ MPa, $\nu_0 = 0.25$) with cracks filled with water ($\kappa = 0.5 \times 10^{-3}$ MPa^{-1}); III—cracks filled with an incompressible fluid ($\kappa = 0$).

$$E_1 = E_2 = E_0, \quad \nu_{12} = \nu_{21} = \nu_0, \quad G_{12} = \frac{E_1}{2(1+\nu_{12})}, \quad \nu_{13} = \nu_{23} = \frac{E_1}{E_3}\nu_{31}. \tag{45}$$

Influence of fluid on the directional variation of Young's modulus may be quite strong (Fig. 7).

For *randomly* oriented crack-like cavities (with aspect ratios uncorrelated with orientations), tensors (40) are isotropic and hence can be found as outlined in Appendix B. The potential is again expressed in terms of two scalar parameters (43):

$$\Delta f = \frac{16(1-\nu_0^2)}{45(2-\nu_0)E_0}\left\{[(5-\nu_0)\rho - 2(1-\nu_0/2)\rho_1]tr(\boldsymbol{\sigma}\cdot\boldsymbol{\sigma}) - \left[\frac{\nu_0}{2}\rho + (1-\nu_0/2)\rho_1\right](tr\boldsymbol{\sigma})^2\right\} \tag{46}$$

and the isotropic effective moduli are

$$\frac{E_0}{E} = 1 + \frac{16(1-\nu_0^2)}{45(2-\nu_0)}[(10-3\nu_0)\rho - 3(2-\nu_0)\rho_1],$$
$$\frac{G_0}{G} = 1 + \frac{16(1-\nu_0)}{45(2-\nu_0)}[(5-\nu_0)\rho - (2-\nu_0)\rho_1]. \tag{47}$$

We emphasize that these expressions for the moduli cannot be reduced to functions of the conventional crack density parameter ρ *only*—ρ_1 is also needed. The case, when all cavities have the same aspect ratio ζ, so that all $\delta^{(k)}$ are the same for all cracks, is the exception: if this (too restrictive, for most applications) assumption is made, the effective moduli can be represented in terms of ρ only. This special case appears to be an implicit assumption in the work of Budiansky and O'Connell (1976).

(3) *Somewhat deformed spheres* $|1-\zeta| \ll 1$. Retaining the terms of the first order in $(1-\zeta)^{(k)}$, we obtain

$$\Delta f = \frac{3(1-\nu_0)}{4E_0}\left\{\left[\frac{4(1+\nu_0)}{7-5\nu_0}\left(\frac{17-35\nu_0}{7(7-5\nu_0)}+\frac{1}{3(1+\delta)}\right)\frac{1}{V}\sum V_{cav}^{(k)}(1-\zeta)^{(k)}\right.\right.$$
$$\left.-\left(\frac{1+5\nu_0}{7-5\nu_0}+\frac{1}{3(1+\delta)}\right)p\right](tr\boldsymbol{\sigma})^2$$
$$+\frac{10(1+\nu_0)}{7-5\nu_0}\left[p-\frac{4(5-7\nu_0)}{7(7-5\nu_0)}\frac{1}{V}\sum V_{cav}^{(k)}(1-\zeta)^{(k)}\right]tr(\boldsymbol{\sigma}\cdot\boldsymbol{\sigma})$$
$$-\frac{4(1+\nu_0)}{7-5\nu_0}\left[\frac{3(17-35\nu_0)}{7(7-5\nu_0)}+\frac{1}{1+\delta}\right](tr\boldsymbol{\sigma})\boldsymbol{\sigma}:\frac{1}{V}\sum[V_{cav}(1-\zeta)\mathbf{nn}]^{(k)}$$
$$\left.+\frac{120(1+\nu_0)(5-7\nu_0)}{7(7-5\nu_0)^2}(\boldsymbol{\sigma}\cdot\boldsymbol{\sigma}):\frac{1}{V}\sum[V_{cav}(1-\zeta)\mathbf{nn}]^{(k)}\right\}. \tag{48}$$

Potential (48) implies the following density parameters: two scalars and one second rank symmetric tensor:

$$p,\quad (1/V)\Sigma V_{cav}^{(k)}(1-\zeta)^{(k)},\quad (1/V)\Sigma[V_{cav}(1-\zeta)\mathbf{nn}]^{(k)}. \tag{49}$$

An interesting observation is that, in the case of *random orientations*, various perturbation terms in (48) cancel out, so that the effective properties are the same as in the case of perfect spheres. Thus, the impact of the shape perturbations on the effective moduli shows up only in second order terms. This explains the fact that, in the case of random orientations, the influence of shape distortions can be neglected up to moderate values of $(1-\zeta)$, see discussion of Section 4. A similar finding for the 2-D case of dry moderately non-circular shapes was reported by Kachanov (1993).

(4) *Needle-shaped cavities* (aspect ratio $\zeta = a_3/a \gg 1$). The potential takes the form:

$$\Delta f = \frac{1}{2E_0}\left\{p4(1-\nu_0^2)tr(\boldsymbol{\sigma}\cdot\boldsymbol{\sigma})-p\left[1-2\nu_0^2+\frac{1}{1+\delta}\frac{(2-\nu_0)^2}{5-4\nu_0}\right](tr\boldsymbol{\sigma})^2\right.$$
$$+2(1+\nu_0)\left[1-2\nu_0-\frac{1}{1+\delta}\frac{2-\nu_0}{5-4\nu_0}\right](tr\boldsymbol{\sigma})\boldsymbol{\sigma}:\frac{1}{V}\sum(V_{cav}\mathbf{nn})^{(k)}$$
$$-4(1-2\nu_0)(1+\nu_0)(\boldsymbol{\sigma}\cdot\boldsymbol{\sigma}):\frac{1}{V}\sum(V_{cav}\mathbf{nn})^{(k)}$$
$$\left.-(1+\nu_0)\left[2\nu_0+\frac{1}{1+\delta}\frac{1+\nu_0}{5-4\nu_0}\right]\boldsymbol{\sigma}:\frac{1}{V}\sum(V_{cav}\mathbf{nnnn})^{(k)}:\boldsymbol{\sigma}\right\}. \tag{50}$$

The structure of (50) implies the following proper density parameters for needles: a scalar and two "porosity tensors", of the second and fourth ranks

$$p\text{-porosity},\quad \frac{1}{V}\sum(V_{cav}\mathbf{nn})^{(k)},\quad \frac{1}{V}\sum(V_{cav}\mathbf{nnnn})^{(k)}. \tag{51}$$

We note an important difference between cracks and the cases of needles and deformed spheres. For cracks, the density parameters contain the fluid compressibility (via $\delta^{(k)}$, see (40_3)). This reflects the fact that the aspect ratios, although small, are generally different for different cracks, and these differences may strongly affect the individual crack contributions into the overall properties. For both needles and deformed spheres, the density parameters (51) and (49), respectively, are *purely geometrical* (do not contain any reference to fluid). This reflects the fact that, although the fluid *does* influence the individual cavity contributions into the overall property, this influence is the same for all cavities (does not

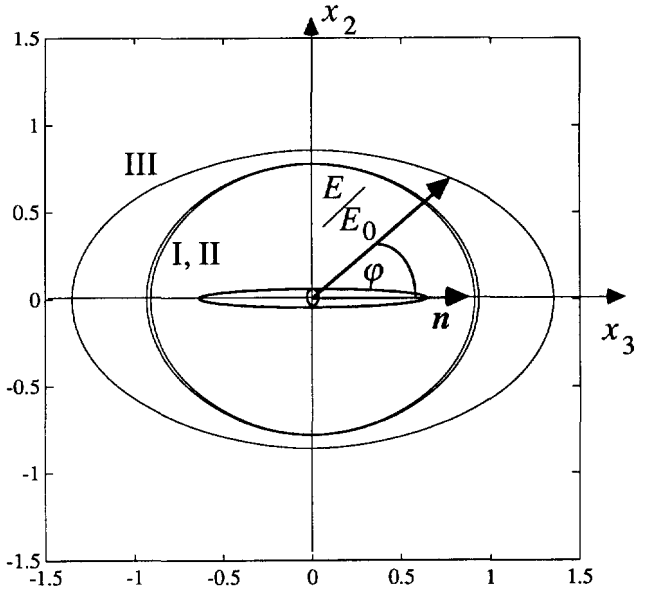

Fig. 8. Parallel needle-shaped cavities (porosity $p = 0.1$). Variation of the effective Young's modulus with direction. I—dry material; II—granite ($E_0 = 6 \times 10^4$ MPa, $\nu_0 = 0.25$) with cavities filled with water ($\kappa = 0.5 \times 10^{-3}$ MPa^{-1}); III—cavities filled with an incompressible fluid ($\kappa = 0$).

depend on the individual $\zeta^{(k)}$, to within small values of the first order). Therefore, $\delta^{(k)} \equiv \delta$ are the same for all cavities and can be taken out of the summation signs, leaving purely geometrical quantities as the density parameters. (This statement is to be revised if some of the cavities are either dry or filled with fluid only partially—for these cavities, the corresponding $\delta^{(k)} = \infty$; see Section 7.)

We examine now the cases of parallel and randomly oriented needles. In yet another contrast with the case of cracks, porosity p becomes a single cavity density parameter in both these cases, and potential Δf is proportional to p.

For *parallel* needles (with the needle axes parallel to the x_3-axis):

$$\Delta f = p\frac{1}{2E_0}\left\{-\left[1-2\nu_0^2+\frac{1}{1+\delta}\frac{(2-\nu_0)^2}{5-4\nu_0}\right](tr\boldsymbol{\sigma})^2+4(1-\nu_0^2)tr(\boldsymbol{\sigma}\cdot\boldsymbol{\sigma})\right.$$
$$+2(1+\nu_0)\left[1-2\nu_0-\frac{1}{1+\delta}\frac{2-\nu_0}{5-4\nu_0}\right]\sigma_{ii}\sigma_{33}$$
$$\left.-4(1-2\nu_0)(1+\nu_0)\sigma_{3j}\sigma_{j3}-(1+\nu_0)\left[2\nu_0+\frac{1}{1+\delta}\frac{1+\nu_0}{5-4\nu_0}\right]\sigma_{33}^2\right\} \quad (52)$$

and the transversely isotropic effective moduli are:

$$\frac{E_0}{E_3} = 1+p\left[1-\frac{1}{1+\delta}\frac{9}{5-4\nu_0}\right], \quad \frac{E_0}{E_1}=\frac{E_0}{E_2} = 1+p\left[3-2\nu_0^2-\frac{1}{1+\delta}\frac{(2-\nu_0)^2}{5-4\nu_0}\right] \quad (53)$$

$$\nu_{31} = \frac{E_3}{E_0}\left[\nu_0+p\left(\nu_0+\frac{1}{1+\delta}\frac{(2-\nu_0)(4+\nu_0)}{5-4\nu_0}\right)\right] \quad (54)$$

$$\nu_{12}=\nu_{21}=\frac{E_1}{E_0}\left[\nu_0+p\left(1-2\nu_0^2+\frac{1}{1+\delta}\frac{(2-\nu_0)^2}{5-4\nu_0}\right)\right], \quad G_0/G_{13}=G_0/G_{23}=1+2p. \quad (55)$$

Figure 8 illustrates the influence of fluid on the directional variation of Young's modulus.

For *randomly oriented* needles (with aspect ratios uncorrelated with orientations), porosity tensors (51) are isotropic. Calculating them as outlined in Appendix B, we obtain

$$\Delta f = p\frac{1}{30E_0}\left\{\left[8\nu_0^2-12\nu_0-5-\Delta_1\frac{1}{1+\delta}\right](tr\boldsymbol{\sigma})^2+\left[8(1+\nu_0)(5-3\nu_0)-\Delta_2\frac{1}{1+\delta}\right]tr(\boldsymbol{\sigma}\cdot\boldsymbol{\sigma})\right\} \tag{56}$$

where it is denoted $\Delta_1 = [5(2-\nu_0)(4-5\nu_0)+(1+\nu_0)^2]/(5-4\nu_0)$, $\Delta_2 = 2(1+\nu_0)^2/(5-4\nu_0)$. The isotropic effective moduli are as follows:

$$\frac{E_0}{E} = 1+p\frac{1}{15}\left[35+4\nu_0-16\nu_0^2-(\Delta_1+\Delta_2)\frac{1}{1+\delta}\right],$$

$$\frac{G_0}{G} = 1+p\frac{1}{15}\left[4(5-3\nu_0)-\frac{1+\nu_0}{5-4\nu_0}\frac{1}{1+\delta}\right]. \tag{57}$$

6. MIXTURES OF CAVITIES OF DIVERSE SHAPES

Pores in real materials may be of diverse shapes; in addition, some of them may be either dry or filled with fluid only partially. Our results cover such situations in a unified way.

As a relatively simple example, we consider a mixture of spheres (of porosity p) and crack-like cavities, both filled with compressible fluid. This case can be viewed as a simple model of a porous microcracked material. Utilizing potentials (37) and (39), we obtain:

$$\Delta f = p\frac{3(1-\nu_0)}{4E_0}\left\{\frac{10(1+\nu_0)}{7-5\nu_0}tr(\boldsymbol{\sigma}\cdot\boldsymbol{\sigma})-\left[\frac{1+5\nu_0}{7-5\nu_0}+\frac{1}{1+\delta_s}\frac{1}{3}\right](tr\boldsymbol{\sigma})^2\right\}$$
$$+\frac{16(1-\nu_0^2)}{3(2-\nu_0)E_0}\left[(\boldsymbol{\sigma}\cdot\boldsymbol{\sigma}):\frac{1}{V}\sum(a^3\mathbf{nn})^{(k)}-\frac{\nu_0}{2}\boldsymbol{\sigma}:\frac{1}{V}\sum(a^3\mathbf{nnnn})^{(k)}:\boldsymbol{\sigma}\right]$$
$$-\frac{8(1-\nu_0^2)}{3E_0}\left[\boldsymbol{\sigma}:\frac{1}{V}\sum\left(\frac{a^3}{1+\delta_c}\mathbf{nnnn}\right)^{(k)}:\boldsymbol{\sigma}\right] \tag{58}$$

where $\delta_s \equiv \delta_{\text{sphere}}$ and $\delta_c \equiv \delta_{\text{crack}}$ are given by (10) and (11). The structure of this potential identifies tensors (40) for cracks plus one scalar—porosity p—as proper density parameters.

For *parallel* cracks ($\mathbf{n} = \mathbf{e}_3$) *mixed with spherical pores*, the potential takes the form:

$$\Delta f = \frac{16(1-\nu_0^2)}{3(2-\nu_0)E_0}\left\{\rho\sigma_{3j}\sigma_{j3}-\left[\frac{\nu_0}{2}\rho+(1-\nu_0/2)\rho_1\right]\sigma_{33}^2\right\}$$
$$+p\frac{3(1-\nu_0)}{4E_0}\left\{\frac{10(1+\nu_0)}{7-5\nu_0}tr(\boldsymbol{\sigma}\cdot\boldsymbol{\sigma})-\left[\frac{1+5\nu_0}{7-5\nu_0}+\frac{1}{1+\delta_s}\frac{1}{3}\right](tr\boldsymbol{\sigma})^2\right\} \tag{59}$$

implying that the set of proper density parameters reduces to three scalars: ρ and ρ_1 defined by (43) plus porosity p. The transversely isotropic effective moduli are:

$$\frac{E_0}{E_3} = 1+\frac{16}{3}(1-\nu_0^2)[\rho-\rho_1]+p\left[\frac{3(1-\nu_0)(9+5\nu_0)}{2(7-5\nu_0)}-\frac{1-\nu_0}{2(1+\delta_s)}\right] \tag{60}$$

$$\frac{E_0}{E_1} = \frac{E_0}{E_2} = 1+p\left[\frac{3(1-\nu_0)(9+5\nu_0)}{2(7-5\nu_0)}-\frac{1-\nu_0}{2(1+\delta_s)}\right] \tag{61}$$

$$\nu_{31}=\frac{E_3}{E_0}\left\{\nu_0+p\frac{1-\nu_0}{2}\left[\frac{3(1+5\nu_0)}{(7-5\nu_0)}+\frac{1}{1+\delta_s}\right]\right\},\quad \frac{G_0}{G_{13}}=1+\rho\frac{8(1-\nu_0)}{3(1-\nu_0/2)}+p\frac{15(1-\nu_0)}{2(7-5\nu_0)} \tag{62}$$

$$\nu_{12}=\nu_{21}=\frac{E_1}{E_0}\left\{\nu_0+p\frac{1-\nu_0}{2}\left[\frac{3(1+5\nu_0)}{(7-5\nu_0)}+\frac{1}{1+\delta_s}\right]\right\},$$

$$G_{12}=\frac{E_1}{2(1+\nu_{12})},\quad \nu_{13}(=\nu_{23})=\frac{E_1}{E_3}\nu_{31}. \tag{63}$$

Note that the presence of spherical pores reduces the degree of anisotropy due to cracks.

For *randomly oriented* cracks (with an additional, compared to the case of *dry* cracks, requirement that crack orientations are uncorrelated with aspect ratios) *mixed with spheres*

$$\Delta f=\frac{1-\nu_0^2}{E_0}\left[p\frac{30}{4(7-5\nu_0)}+\rho\frac{16(5-\nu_0)}{45(2-\nu_0)}-\rho_1\frac{16}{45}\right]tr(\boldsymbol{\sigma}\cdot\boldsymbol{\sigma})$$

$$-\frac{1-\nu_0}{E_0}\left\{p\left[\frac{3(1+5\nu_0)}{4(7-5\nu_0)}+\frac{1}{1+\delta_s}\frac{1}{4}\right]+\frac{8(1+\nu_0)}{45}\left[\frac{\nu_0}{2-\nu_0}\rho+\rho_1\right]\right\}(tr\boldsymbol{\sigma})^2. \tag{64}$$

Strictly speaking, the structure of (64) implies two independent scalar density parameters (in agreement with the general structure (34))—coefficients at $(tr\boldsymbol{\sigma})^2$ and $tr(\boldsymbol{\sigma}\cdot\boldsymbol{\sigma})$; it is more convenient to express the effective moduli in terms of three scalars ρ, ρ_1 and p that have clear physical meaning (ρ and p are the usual crack density and porosity, and $\rho_1=0$ for dry cavities).

$$\frac{E_0}{E}=1+\frac{16(1-\nu_0^2)}{45(2-\nu_0)}[(10-3\nu_0)\rho-3(2-\nu_0)\rho_1]+p\left[\frac{3(1-\nu_0)(9+5\nu_0)}{2(7-5\nu_0)}-\frac{1-\nu_0}{2(1+\delta_s)}\right] \tag{65}$$

$$\frac{G_0}{G}=1+\frac{16(1-\nu_0)}{45(2-\nu_0)}[(5-\nu_0)\rho-(2-\nu_0)\rho_1]+p\frac{15(1-\nu_0)}{2(7-5\nu_0)}. \tag{66}$$

Figure 9 shows the dependence of the effective Young's modulus on the crack density, at the given "background" porosity $p=0.1$, for several aspect ratios ζ of the crack-like cavities (assumed to be the same for all cracks).

7. EFFECTIVE ANISOTROPY AS DETERMINED BY THE PROPER CAVITY DENSITY PARAMETERS

One of the advantages of the proper defect density parameters is that their identification establishes the anisotropy of the overall properties. We discuss, from this standpoint, the results obtained above. The discussion is summarized in Table 1.

(1) *Narrow, crack-like cavities.* This case is described by potential (39), or by approximate simplified potential (41).

We first discuss the approximate formulation (41). The first term corresponding to a *dry* solid contains crack density tensor $\boldsymbol{\alpha}=(1/V)\Sigma(a^3\mathbf{nn})^{(k)}$. Since it is a symmetric second rank tensor, the effective elastic properties possess the symmetry of an ellipsoid, i.e., a dry solid with cracks which are *orthotropic*, for any arbitrary orientational distribution of cracks. This result is non-trivial and may be counterintuitive: it applies, for example, to two families of crack-like cavities inclined at an arbitrary angle to each other. Moreover, the orthotropy is of a special, simplified type: (1) the number of independent elastic constants is reduced from 9 to 4 and (2) the variation of Young's modulus with direction

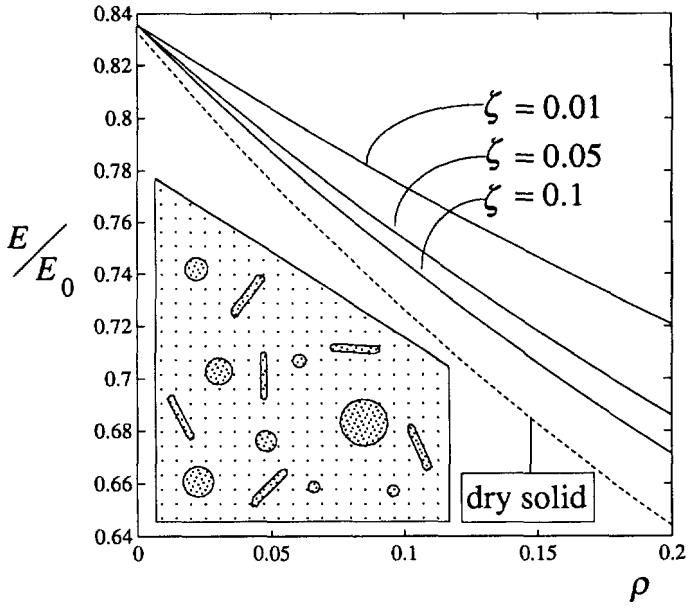

Fig. 9. Mixtures of spheres (porosity $p = 0.1$) and randomly oriented crack-like cavities of the same aspect ratio ζ. Dependence of the effective Young's modulus on the crack density ρ (for several aspect ratios ζ, the same for all cavities). Material parameters correspond to granite ($E_0 = 6 \times 10^4$ MPa, $\nu_0 = 0.25$) filled with water ($\kappa = 0.5 \times 10^{-3}$ MPa^{-1}).

is described by an ellipsoid, rather than by a 4-th order surface (for a detailed discussion, see Kachanov 1980, 1992). The second term (due to fluid) contains a fourth rank tensor $(1/V)\Sigma[a^3(1+\delta)^{-1}\mathbf{nnnn}]^{(k)}$ that, generally, causes deviations from orthotropy. For a *dry* solid, a similar term in (41) containing fourth rank tensor $(1/V)\Sigma(a^3\mathbf{nnnn})^{(k)}$ can be neglected, as discussed in Section 5, and the orthotropy is not violated.

If fluid is present, the second term in (41) cannot, generally, be neglected, except for the case when parameters $\delta^{(k)}$ are large (highly compressible fluid or very stiff matrix). Therefore, for a solid with fluid inclusions, the orthotropy for an arbitrary orientational distribution does not hold.

(2) *Somewhat deformed spheres.* The potential (48) is correct to within values of the first order in $(1-\zeta)$. Its structure implies that the set of proper density parameters consists of two scalars (see the coefficients at $(tr\boldsymbol{\sigma})^2$ and $tr(\boldsymbol{\sigma}\cdot\boldsymbol{\sigma})$) and one symmetric second rank tensor. Therefore, a simplified orthotropy holds (similarly to the case of a dry solid with cracks).

(3) *Needle-shaped spheroids.* This case is characterized by the potential (50). Its structure identifies one scalar (porosity p) and two tensors of the second and fourth ranks (51) as the proper density parameters. Since the two tensors are, generally, not coaxial, the effective elastic properties of a solid with a general non-random orientational distribution of needles may possess no symmetry elements, even in the case of a *dry* solid (in contrast with a dry solid with *cracks*, which is orthotropic). The case of *randomly oriented* needles, on the other hand, is simpler than the one of randomly oriented cracks: the only density parameter is porosity p (vs two scalar parameters, ρ and ρ_1, for fluid-filled cracks).

(4) *General spheroids.* The structure of the potential (33) implies that the set of proper density parameters consists of two scalars—coefficients at $(tr\boldsymbol{\sigma})^2$ and $tr(\boldsymbol{\sigma}\cdot\boldsymbol{\sigma})$, two non-coaxial symmetric second rank tensors—coefficients at $(tr\boldsymbol{\sigma})\boldsymbol{\sigma}$: and $(\boldsymbol{\sigma}\cdot\boldsymbol{\sigma})$: and one fourth rank tensor (in the last term of (33)). No elements of elastic symmetry exist in the case of general orientational distribution.

On correct interpretation of experimental data on elasticity of porous materials

The use of proper cavity density parameters is essential for a correct interpretation of experimental data on elasticity of porous materials. As discussed in Section 5, even in the case of overall isotropy (random orientation) the density parameters are non-trivial and do

Table 1. Cavity density parameters and effective anisotropies for dry and fluid-filled spheroidal cavities

Geometry $a_1 = a_2 \equiv a$ $\zeta \equiv a_3/a$	Arbitrary orientational distribution				Random orientations (isotropy)	
	Cavity density parameters		Anisotropy		Cavity density parameters (scalars)	
	dry cavities	fluid-filled cavities	dry cavities	fluid-filled cavities	dry cavities	fluid-filled cavities
Narrow, crack-like cavities $\zeta \ll 1$	1) Symmetric 2nd rank crack density tensor $\boldsymbol{\alpha} = (1/V)\Sigma[a^3\mathbf{nn}]^{(k)}$ 2) Fully symmetric 4th rank tensor (plays a minor role) $1/V\Sigma[a^3\mathbf{nnnn}]^{(k)}$	Same as for dry cracks plus $(1/V)\Sigma[a^3(1+\delta)^{-1}\mathbf{nnnn}]^{(k)}$	Simplified orthotropy (approx., accuracy depends on ν_0)	General anisotropy	Crack density $\rho = (1/V)\Sigma[a^3]^{(k)}$	Same as for dry cracks plus $\rho_1 = (1/V)\Sigma[a^3(1+\delta)]^{(k)}$
Spheres	Porosity $p = (1/V)\Sigma V_{cav}^{(k)}$	Same as for dry spheres	Isotropy	Isotropy	p	p
Somewhat deformed spheres $\lvert 1-\zeta\rvert \ll 1$	1) p 2) Scalar $(1/V)\Sigma[V_{cav}(1-\zeta)]^{(k)}$ 3) Symmetric 2nd rank tensor $(1/V)\Sigma[V_{cav}(1-\zeta)\mathbf{nn}]^{(k)}$	Same as for dry deformed spheres	Simplified orthotropy, to within first order in $1-\zeta$	Simplified orthotropy, to within first order in $1-\zeta$	p	p
Needles $\zeta \gg 1$	1) p 2) Symmetric 2nd rank tensor $(1/V)\Sigma[V_{cav}\mathbf{nn}]^{(k)}$ 3) Fully symmetric 4th rank tensor $(1/V)\Sigma[V_{cav}\mathbf{nnnn}]^{(k)}$	Same as for dry needles	General anisotropy	General anisotropy	p	p
General spheroids	General anisotropy, for both dry and fluid-filled cavities. For the proper density parameters (different for dry and fluid-filled pores), see formula (33) and text.				Scalars p_1, p_2, given by (35) with $\delta^{(k)} = \infty$	Scalars p_1, p_2, given by (35)

not, generally, reduce to porosity. Therefore, if the shape factors are ignored, the attempts to estimate porosity from the data on the effective moduli may yield grossly exaggerated values, particularly in the case of oblate shapes. This was discussed by Kachanov *et al.* (1994) in connection with *dry* porous ceramics. For materials with *fluid-filled* cavities, the shape factors enter in combination with physical parameter $\delta^{(k)}$. The results of the present work provide all the ingredients for a correct interpretation of experimental data.

Partially saturated materials

One of the advantages of proper cavity density parameters, that correctly take the individual cavity contributions, is that they cover the important case of partially saturated materials (some of the cavities are dry or filled with fluid only partially). The presence of dry cavities is accounted for by taking the corresponding $\delta^{(k)} = \infty$. This also applies to cavities that are only partially filled with fluid, if the compressibility of the gas that fills the remaining part of a cavity is much higher than the one of the fluid.

Table 1, summarizing the discussion of this section, is restricted to spheroidal geometries. As far as the general ellipsoidal shapes are concerned, the proper parameters of defect density directly follow from substitution of the expressions (17) and (19) for $\mathbf{H}$ and $\Delta\mathbf{H}$ into the potential (31). Such a substitution yields exact expressions for Δf and the density parameters in terms of Eshelby's tensor. These, rather lengthy, expressions are not included in the table.

The table also assumes that cavities are *fully* filled with fluid. If some of the cavities are either *partially* filled or dry, their individual contributions to the overall density parameters are taken with $\delta^{(k)} = \infty$, and the results are to be modified as outlined above.

The term "simplified orthotropy" used in Table 1 is discussed above in this section. We also note that summation over cavities in the density parameters can be replaced by integration over orientations, see (32).

Acknowledgments—The authors thank Dr Zimmerman for a number of useful comments. This work was supported by the Army Research Office through a grant to Tufts University. The second author (MK) was also supported by von Humboldt research award for senior scientists.

REFERENCES

Budiansky, B. and O'Connell, R. J. (1976). Elastic moduli of a cracked solid. *International Journal of Solids and Structures* **12,** 81–97.

Eshelby, J. D. (1957). The determination of the elastic field of an ellipsoidal inclusion and related problems. *Proceedings of the Royal Society* **A241,** 376–396.

Fung, Y. C. (1994). *A First Course in Continuum Mechanics*, 3rd edn, Prentice Hall, Englewood Cliffs, New Jersey, U.S.A.

Hill, R. (1963). Elastic properties of reinforced solids: some theoretical principles. *Journal of Mechanics and Physics of Solids* **11,** 357–372.

Kachanov, M. (1980). Continuum model of medium with cracks. *Journal of the Engineering Mechanics Division* **106,** 1039–1051.

Kachanov, M. (1982). Microcrack model of rock inelasticity. Part I: frictional sliding on pre-existing microcracks. *Mechanics of Materials* **1,** 1–19.

Kachanov, M. (1992). Effective elastic properties of cracked solids: critical review of some basic concepts. *Applied Mechanics Reviews* **45,** 304–335.

Kachanov, M. (1993). Elastic solids with many cracks and related problems. In *Advances in Applied Mechanics*, Vol. 30 (eds Hutchinson, J. W. and Wu, T. Y.), Academic Press, Boston, MA, pp. 259–445.

Kachanov, M., Tsukrov, I. and Shafiro, B. (1994). Effective moduli of solids with cavities of various shapes. *Applied Mechanics Reviews* **47,** S151–S174.

Kachanov, M., Tsukrov, I. and Shafiro, B. (1995). Materials with fluid-saturated cracks and cavities: fluid pressure polarization and effective elastic response. *International Journal of Fracture* (*Reports of Current Research*) **73,** R61–R66.

Mura, T. (1987). *Micromechanics of Defects in Solids*, 2nd edn, Kluwer Academic Publishers, Dordrecht, The Netherlands.

O'Connell, R. J. and Budiansky, B. (1974). Seismic velocities in dry and saturated cracked solids. *Journal of Geophysics Research* **79,** 5412–5426.

Tsukrov, I. and Kachanov, M. (1993). Solids with holes of irregular shapes: effective moduli and anisotropy. *International Journal of Fracture* (*Reports of Current Research*) **64,** R9–R12.

Vavakin, A. S. and Salganik, R. L. (1975). Effective characteristics of nonhomogeneous media with isolated inhomogeneities. *Izv. ANSSR, Mekhanika Tverdogo Tela* **10,** 65–75 (in Russian); English translation *Mechanics of Solids*, pp. 58–66.

Zimmerman, R. (1991). *Compressibility of Sandstones*, Elsevier Science Publishers, Amsterdam, The Netherlands.

APPENDIX A

Components of the cavity compliance tensor **H** *for a general ellipsoidal cavity*

$$H_{1111} = \frac{V_{cav}}{V}\frac{1}{E_0}\frac{1}{\Delta}\{(1-S_{2222})(1-S_{3333}) - S_{2233}S_{3322}$$
$$-\nu_0[S_{1122}(1-S_{3333}+S_{2233}) + S_{1133}(1-S_{2222}+S_{3322})]\}$$
$$H_{1122} = \frac{V_{cav}}{V}\frac{1}{E_0}\frac{1}{\Delta}\{S_{1122}(1-S_{3333}) + S_{1133}S_{3322}$$
$$-\nu_0[(1-S_{2222})(1-S_{3333}+S_{1133}) + S_{2233}(S_{1122}-S_{3322})]\}$$
$$H_{1212} = \frac{V_{cav}}{V}\frac{1}{E_0}\frac{1+\nu_0}{2(1-2S_{1212})}, \quad \Delta = -\mathrm{Det}\begin{bmatrix} S_{1111}-1 & S_{1122} & S_{1133} \\ S_{2211} & S_{2222}-1 & S_{2233} \\ S_{3311} & S_{3322} & S_{3333}-1 \end{bmatrix}$$

where $V_{cav} = (4/3)\pi a_1 a_2 a_3$, S_{ijkl} are components of Eshelby's tensor. The remaining H_{ijkl} are obtained by the cyclic permutation of (1, 2, 3). For a general ellipsoid, S_{ijkl} are expressed in terms of elliptic integrals (Eshelby, 1957); for a spheroid, they can be reduced to elementary functions (Mura, 1987).

Coefficients A_i *and* B_i *for a general spheroid (entering the pressure polarization tensor* (9)*, the compliance tensors* (19)–(21) *and the potential* (33))

Here, x_3 is the symmetry axis of the spheroid and Δ is defined above.

$$A_1 = \frac{1}{\Delta}\{(1-S_{3333}+S_{1133})[S_{1122}-\nu_0(1-S_{1111})] - (1+\nu_0)S_{1133}(S_{1122}-S_{3311})\}$$
$$A_2 = \frac{1+\nu_0}{2(1-2S_{1212})}, \quad A_4 = 2(1+\nu_0)\left[\frac{1}{(1-2S_{1313})} - \frac{1}{(1-2S_{1212})}\right]$$
$$A_3 = \frac{2}{\Delta}\{(1-S_{1111}+S_{1122})[(1-\nu_0)S_{3311}+\nu_0(S_{1111}+S_{1122}+S_{1133}-1)]$$
$$+(1-S_{3333})[\nu_0(1-S_{1111})-S_{1122}] - (1+\nu_0)S_{1133}S_{3311}\}$$
$$A_5 = \frac{1}{\Delta}\{(1-S_{1111}+S_{1122})[(1+2\nu_0)(1-S_{1111}-S_{1122}) - 2S_{3311}]$$
$$-(1+\nu_0)S_{1133}(1-S_{1111}+S_{3311}) + (1-S_{3333}+S_{1133})(1-S_{1111}-\nu_0 S_{1122})\} - \frac{2(1+\nu_0)}{(1-2S_{1313})}$$
$$B_1 = \frac{3}{2}A_3 + A_4 + A_5, \quad B_2 = 3A_1 + A_2 + \frac{1}{2}A_3, \quad B_3 = \frac{1}{R}B_2^2, \quad B_4 = \frac{1}{R}B_1 B_2, \quad B_5 = \frac{1}{R}B_1^2.$$

APPENDIX B

Calculation of isotropic fully symmetric tensors in terms of their traces (relevant for randomly oriented cavities, formulas (34, 48, 58)).

We consider tensors of the second and fourth ranks: $(1/V)\Sigma(C\mathbf{nn})^{(k)}$ and $(1/V)\Sigma(D\mathbf{nnnn})^{(k)}$, where $C^{(k)}$ and $D^{(k)}$ are certain scalars associated with k-th cavity. In the case when these tensors are known to be *isotropic* (random orientations, with distributions of $C^{(k)}$ and $D^{(k)}$ uncorrelated with orientations), they can be evaluated as follows.

The second rank tensor $(1/V)\Sigma(C\mathbf{nn})^{(k)}$, being isotropic, is proportional to the unit tensor, i.e., is equal to $c\mathbf{I}$. To determine c, we take the linear invariant of the equation $(1/V)\Sigma(C\mathbf{nn})^{(k)} = c\mathbf{I}$. Then, since $tr\mathbf{I} = 3$,

$$(1/V)\sum(C\mathbf{nn})^{(k)} = \frac{1}{3V}[\Sigma C^{(k)}]\mathbf{I}.$$

If the fourth rank tensor $(1/V)\Sigma(D\mathbf{nnnn})^{(k)}$ is known to be isotropic, its $ijkl$ components are (see, for example, Fung, 1994): $c_1\delta_{ij}\delta_{kl} + c_2(\delta_{ik}\delta_{jl}+\delta_{il}\delta_{jk}) + c_3(\delta_{ik}\delta_{jl}-\delta_{il}\delta_{jk})$ where c_1, c_2, c_3 are some constants. Since, in addition to being isotropic, the tensor is fully symmetric with respect to all rearrangements of indices (as a sum of fully symmetric tensors), $c_3 = 0$ and $c_1 = c_2 \equiv c$. The constant c can be determined in terms of the sum $(1/V)\Sigma D^{(k)}$ by the contraction $i = j, k = l$: $(1/V)\Sigma(D\mathbf{n}\cdot\mathbf{nn}\cdot\mathbf{n})^{(k)} \equiv (1/V)\Sigma D^{(k)} = 15c$. Thus,

$$\frac{1}{V}\sum(D\mathbf{nnnn})^{(k)} = \frac{1}{15V}[\Sigma D^{(k)}](\mathbf{II}+2\mathbf{J})$$

where $\mathbf{I}$ is the second rank unit tensor and $\mathbf{J} = (\delta_{ik}\delta_{jl}+\delta_{il}\delta_{jk})\mathbf{e}_i\mathbf{e}_j\mathbf{e}_k\mathbf{e}_l$.